Food Hydrocolloids 172 (2026) 111991

Contents lists available at ScienceDirect

Food Hydrocolloids

journal homepage: www.elsevier.com/locate/foodhyd

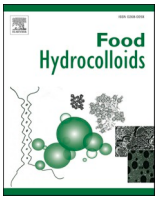

Controlling the cold-set gelation of Bovine Serum Albumin protein using alcohol and ionic surfactant

Debasish Saha [a,*,1], Sugam Kumar [b,c,**,1], Purushottam S. Dubey [a], Jitendra P. Mata [d,e], Andrew E. Whitten [d], Joachim Kohlbrecher [f], Henrich Frielinghaus [a], Vinod K. Aswal [b,c]

[a] Juelich Centre for Neutron Science-4, Forschungszentrum Juelich, Juelich, 52425, Germany
[b] Solid State Physics Division, Bhabha Atomic Research Centre, Mumbai, 400 085, India
[c] Homi Bhabha National Institute, Mumbai, 400 094, India
[d] Australian Centre for Neutron Scattering (ACNS), Australian Nuclear Science and Technology Organization (ANSTO), Lucas Heights, NSW, 2234, Australia
[e] School of Chemistry, University of New South Wales, Sydney, NSW, 2052, Australia
[f] PSI Center for Neutron and Muon Sciences, Paul Scherrer Institut, 5232, Villigen PSI, Switzerland

ARTICLE INFO

Keywords:
BSA protein
Cold gelation of BSA
Inhibition of gelation
SANS
Rheology
Interplay of interactions

ABSTRACT

Heating of globular protein solutions usually leads to protein denaturation and subsequent gelation at high temperatures. Under "cold gelation", protein forms a gel at a much lower temperature than its original gelation temperature (T_G), which can be achieved by modifying various physicochemical conditions such as the pH of the solution, the presence of salts, etc. In this study, we investigated the cold gelation of Bovine Serum Albumin (BSA) protein induced by ethanol and controlled by ionic surfactant, using small-angle neutron scattering (SANS), dynamic light scattering (DLS), and rheology The results show that the T_G of the protein with ethanol is systematically decreased as compared to the that of pure BSA solutions (~80 °C), reaching ~60 °C at 10 wt% ethanol, ~55 °C at 20 wt% and finally as low as ~38 °C in presence of 30 wt% ethanol in the solution. Rheological measurements demonstrate a significant strengthening of the gel network, with the enhancement in storage modulus (G′) from ~20 Pa at 0 wt% to ~250 Pa at 30 wt% ethanol. Structural characterization reveals an increase in fractal dimension with rising ethanol content, indicating denser and more branched gel networks. Interestingly, the addition of the anionic surfactant sodium dodecyl sulfate (SDS) inhibits the alcohol-assisted cold gelation of BSA protein, depending upon the relative amount of ethanol and SDS in solution. The results are explained based on the interplay of interactions in the protein, manipulated by the presence of alcohol, elevated temperatures, and ionic surfactant. Our study highlights the tunability of gelation pathways and offers useful inputs for controlled protein gelation in biomaterial and food industry.

1. Introduction

Increasing the temperature of protein dispersions initiates the denaturation of protein via breaking of hydrogen and disulfide bonds. These denatured proteins undergo hydrophobic attraction due to exposure of the hydrophobic sites of the protein, resulting in the formation of smaller protein aggregates, which finally leads to protein gelation by forming intermolecular network structure at the gelation temperature (T_G) (Clark et al., 2001; Gosal & Ross-Murphy, 2000; Tobitani & Ross-Murphy, 1997). Protein gels can also be obtained at lower relative temperatures through the manipulation of physicochemical conditions such as pH, pressure or the presence of salts, a process called cold-set gelation (Ako et al., 2010; Alting et al., 2004a; Lerch et al., 2024; Liu et al., 2024; Ryu & McClements, 2024; Speroni & Añón, 2013; Tomczyńska-Mleko et al., 2023; Zhao et al., 2021). While the thermal gelation of proteins is well studied, the cold gelation, where proteins form gels at sub-denaturation temperatures, is increasingly relevant for applications where thermal processing is undesirable (Yang et al., 2017). The cold gelation enables energy-efficient processing, preserves the bioactivity of sensitive components, and allows precise tuning of gel texture, making it valuable for food structuring, drug delivery, and tissue engineering (Alting et al., 2004b; Mariz de Avelar

* Corresponding author.
** Corresponding author. Solid State Physics Division, Bhabha Atomic Research Centre, Mumbai 400 085, India.
E-mail addresses: d.saha@fz-juelich.de (D. Saha), sugam@barc.gov.in (S. Kumar).
[1] These authors have equal contributions.

https://doi.org/10.1016/j.foodhyd.2025.111991
Received 6 May 2025; Received in revised form 10 September 2025; Accepted 15 September 2025
Available online 16 September 2025

et al., 2020; Xu et al., 2023). The cold gelation of protein is usually directed via a two-step process. In the initial step, a solution of native proteins is heated up to a temperature lower than the T_G, resulting in the formation of soluble aggregates. Once cooled, these aggregates stay soluble, and gelation does not take place. In the second step, gelation is triggered at lower temperatures by decreasing the electrostatic repulsion, either by adding salt or by adjusting the pH towards the protein's isoelectric point. Nevertheless, these approaches of protein gelation require some amount of heating (Ako et al., 2010; Alting, van der Meulena, et al., 2004).

The temperature-driven enhancement in the hydrophobic attraction and charge dependent electrostatic repulsion between protein molecules largely decides the behavior of the protein solutions on heating. If the repulsion in the system is dominating, the system does not undergo gelation and remain in solution (sol) state. Therefore, the primary condition for achieving cold gelation is to enhance the protein denaturation and suppress the electrostatic repulsion in the system (Clark et al., 2001). Apart from the usual protocol of cold gelation as discussed above, addition of protein denaturing agents may promote the protein gelation even at lower temperatures. For example, addition of oppositely charged surfactant in protein dispersion usually supports its gelation by (i) denaturing the protein and (ii) reducing the electrostatic repulsion (Dubey et al., 2016; Kumar & Aswal, 2024; T. O. Nnyigide et al., 2023). In this context, addition of cosolvents such as alcohol or acids has also been reported to disrupt the secondary structure of the protein and hence enabling the cold-set gelation (Arabi et al., 2020; Kaewprasit et al., 2018; Yoshikawa et al., 2012; Yu et al., 2020). In particular, alcohols is known to induce partial protein unfolding and promote hydrophobic interactions, thus can assist the gelation process (Nikolaidis et al., 2017). Ethanol has been shown to enable cold gelation of whey protein at room temperature, with the extent of gelation strongly dependent on ethanol concentration and solution pH (Nikolaidis & Moschakis, 2018). Furthermore, ethanol can also influence the microstructure and properties of protein gels. For example, acid-induced gels prepared in presence of alcohal exhibit distinct morphological changes (Wagner et al., 2021). Similarly, it has been reported that low ethanol content leads to disulfide bond-driven elastic protein gels, while higher ethanol levels produce weaker gels primarily stabilized by hydrogen bonding and electrostatic interactions (Andlinger et al., 2022). Ethanol pretreatment combined with thermal processing has also been used to develop thermo-reversible gels of whey protein, underscoring the tunability of such systems (Andreadis & Moschakis, 2023b).

It is clear from above examples that ethanol (or alcohols, in general) may induce cold-gelation by modifying both the hydrophobic as well as the electrostatic interactions between protein molecules (Chong et al., 2015). However, tuning of this process has not been well explored. It could be of further interest to inhibit such gelation through other co-solutes (e.g., amphiphiles, multivalent ions etc.), permitting control over the sol-gel transitions, depending on the need of targeted application (Gao et al., 2020; Mercadé-Prieto & Gunasekaran, 2009; Song et al., 2021; Venezia et al., 2022). The inhibition of Bovine Serum Albumin (BSA) protein gelation was achieved in the past by different means such as the excess condensation of multivalents Zr^{+4} ions, or anionic SDS surfactants (Kumar & Aswal, 2024; Kumar et al., 2021, 2023). Unlike cationic surfactants, which accelerate the gelation of BSA protein, sodium dodecyl sulfate (SDS) prevents such gelation although both surfactants work as denaturants for BSA protein at room temperature.

In this work, we examine the ethanol-driven cold-set gelation of BSA protein, where gelation could be achieved at temperatures as low as room temperature. BSA is a widely used model protein due to its well-characterized structure and functional similarities with many food proteins such as ovalbumin, beta-lactoglobulin. The gel formation has been established by both macroscopically, using visual inspection and tube inversion tests and microscopically, using rheology measurements (Rodríguez Patino et al., 1999). We further probed the structural modifications during such gelation using small-angle neutron (SANS) and dynamic light scattering (DLS) techniques (Majcher et al., 2022; Yoshida et al., 2010; Zhu et al., 2022). Interestingly, alcohol-induced cold gelation of protein could be completely suppressed on addition of the ionic surfactant sodium dodecyl sulfate (SDS). The underlying mechanism has been explained based on competing interactions in the presence of alcohol and SDS. It should be noted that the protein, alcohol, and surfactants, are all important components in the food industry and hence the pathways examined in this study can be highly useful in designing and controlling food gels (Boulet et al., 2001; Pizones Ruíz-Henestrosa et al., 2008; Rodríguez Patino et al., 2004; Yaghmur et al., 2002). Insights gained from ethanol-induced gelation and SDS-mediated inhibition of BSA can thus be extended to understand and control the gelation behavior in complex food systems. Moreover, understanding the nanostructure of these gels can provide useful inputs for dictating the properties such as texture, stability, nutrient release, shelf life, etc. (Banc et al., 2016; Bayrak et al., 2023; Cao & Mezzenga, 2020; Napieraj et al., 2022).

2. Experimental

2.1. Materials and sample preparation

BSA protein, sodium dodecyl sulfate (SDS) surfactant, and ethanol were purchased from Sigma-Aldrich. All the chemicals were used as received, without any further purification. The appropriate concentration (4 wt%) of BSA solution was prepared by dissolving the lyophilized BSA powder (as provided by supplier, with no further purification) in 20 mM pH ~7.2 buffer. A D_2O/ethanol mixture was used as a solvent for SANS, whereas an H_2O/ethanol mixture was used as a solvent for other measurements. These solutions were subjected to gentle mixing at room temperature to ensure full hydration and dissolution of the protein. These solutions are heated to obtain the gels. Each sample was equilibrated for approximately 30 min at the specified temperature. All the gels were prepared in 23 mm × 85 mm × 18 mm clear vials for macroscopic and rheological measurements. On the other hand, for SANS and DLS, the samples were gradually heated to the gelation temperature in the cuvettes to monitor the evolution of structure and interactions within the system during the gelation process. The gelation temperatures presented in the manuscript were determined separately by heating the samples in an oil bath. These gelation temperatures are consistent with the structural changes observed via SANS, DLS, and transmission measurements, providing reliable confirmation of the gelation behavior. It should be mentioned here that BSA concentration of 4 wt% was chosen because it yielded a gelation temperature (~80 °C) that provided an optimal experimental window to systematically investigate both ethanol-induced cold gelation and SDS-mediated inhibition (discussed later). This concentration allowed us to clearly observe the progressive lowering of gelation temperature with increasing ethanol concentration (down to ~ 40 °C), as well as the ability of SDS to inhibit gelation even at elevated temperatures (up to ~ 95 °C).

2.2. Methods

2.2.1. Dynamic light scattering (DLS)

DLS measurements were performed using Malvern ZETASIZER Nano series (Nano-S) instrument. The instrument utilizes a laser source of light of wavelength 633 nm while scattered light is measured using Avalanche photodiode detector, placed at 173° angle. Transmission measurements were carried out using nanoparticle size analyzer SZ-100 of Horiba, utilizing a laser light of wavelength 532 nm. DLS and transmission measurements were repeated at least five times to ensure the consistency of the results.

2.2.2. Small-angle neutron scattering (SANS)

Small-angle neutron scattering experiments were performed on the Bilby instrument at the OPAL reactor at ANSTO (Sydney, Australia) and

SANS-I instrument at PSI, Switzerland. The Bilby instrument was configured in a conventional monochromatic pinhole SANS instrument mode at a fixed wavelength (λ) of 6.0 Å with wavelength resolution ($\Delta\lambda/\lambda$) ~ 0.1 (Sokolova et al., 2016). The rear detector was positioned 18.0 m from the sample, and the curtain detector banks were positioned 1.5 m and 2.5 m from the sample, to cover a wave vector transfer ($Q = 4\pi \sin(\theta/2)/\lambda$, where θ is the scattering angle) range of 0.003–0.40 $Å^{-1}$. Same wavelength of neutron (λ = 6.0 Å and $\Delta\lambda/\lambda$ ~ 0.1) were used for the SANS measurement at SANS-I instrument, PSI. A two-dimensional (96 × 96 cm^2) ^{3}He gas detector was used for scattered neutron detection. Two sample-to-detector distances of 2 m and 8 m were used to cover the wave vector transfer Q-range from 0.005 to 0.22 $Å^{-1}$.

The samples were held in Hellma quartz cuvettes (120-QS at Bilby and 404-QX at SANS-I) with 2 mm path length during the SANS measurements. Cuvettes were aligned using the thermostatic sample holder and vary the temperature from 25 °C to 80 °C (as required). The raw data were radially averaged, corrected for electronic background and empty cell and normalized to absolute scale using standard protocol (Arnold et al., 2014; Keiderling, 2002).

2.2.3. Rheology

The storage and loss moduli of the gel samples were measured using Anton Paar Physica MCR92 rheometer employing parallel plate geometry. The gel samples were first prepared by heating the protein solutions with increasing concentration of ethanol in ethanol/water mixtures at respective T_G. All gel samples were prepared in closed vials to avoid the solvent evaporation at higher temperatures. Then rheological characterization was carried out on these samples at room temperature.

2.3. Data analysis

2.3.1. DLS data analysis

Dynamic Light Scattering (DLS) measurements yield the autocorrelation function (ACF) as a function of delay time (τ). These plots are obtained from the fluctuations in the intensity of scattered light, which correlate with the translational diffusion coefficient (D) of particles in suspension. The normalized intensity autocorrelation function, denoted as $g^2(\tau)$, is described by the following relationship (Kaszuba et al., 2008; Lorber et al., 2012; Stetefeld et al., 2016):

$$g^2(\tau) = 1 + \beta\left|e^{-DQ^2\tau}\right|^2 \tag{1}$$

here β denotes the spatial coherence factor, decided by the instrument optics. Q represents the magnitude of wave vector transfer.

In a polydisperse system of narrow size distribution of scatterers, cumulant analysis is typically applied to determine the mean diffusion coefficient. The following Stokes-Einstein relation is then utilized to determine effective mean hydrodynamic diameter (D_h) of the scatterers from mean diffusion coefficient:

$$D_h = \frac{k_B T}{3\pi\eta D} \tag{2}$$

In the above equation, k_B, T, and η denote Boltzmann's constant, absolute temperature, and viscosity of the solvent, respectively.

2.3.2. SANS analysis

Small-angle neutron scattering (SANS) is used to study the structure and interactions of macromolecules (e.g., proteins, surfactants etc.), dispersed in a medium (Gilbert, 2023). In SANS, a beam of monochromatic neutrons is made incident onto the sample, and the intensity of scattered neutrons is measured at different scattering angles. The intensity of the scattered neutrons for a system consisting of monodispersed particles dispersed in a medium can be given by following relation (Jeffries et al., 2021; Li et al., 2016)

$$I(Q) = \frac{N_p(\rho_p - \rho_m)^2 V_p^2}{V_S} P(Q)\, S(Q) \tag{3}$$

where, Q is the magnitude of scattering vector. N_p is the number of scatterers in the sample; V_s represents the sample volume; V_p is the volume of a single scatterer; $(\rho_p - \rho_m)^2$ is called the contrast factor and is scattering length density difference between particle (ρ_p) and matrix (ρ_m); $P(Q)$ is the intraparticle structure factor; $S(Q)$ denotes the interparticle structure factor.

The expression for $P(Q)$ of ellipsoidal particle is given by

$$P(Q) = \int_0^1 F(Q,\mu)^2 d\mu$$

where $F(Q,x) = \frac{3(\sin x - x\cos x)}{x^3}$ in this

$$x = Q\left[a^2\mu^2 + b^2(1-\mu^2)\right]^{\frac{1}{2}} \tag{4}$$

where a and b represent the semi-axes for ellipsoid shape, μ is the cosine of the angle between the direction of major axis and scattering vector Q. The BSA protein is usually described by an oblate ($b = c > a$) ellipsoidal shape (Wang et al., 2023).

$S(Q)$ for an attractive system may be accounted by following square -well potential (Sharma & Sharma, 1977)

$$U(r) = \begin{cases} \infty for\ 0 < r < \sigma \\ -\varepsilon \quad for\ \sigma < r < \sigma + \Delta \\ 0 \quad for\ r > \sigma + \Delta \end{cases} \tag{5}$$

where Δ and ε correspond to the width and the depth of the potential while σ is the hard sphere diameter of the particle/scatterer. The rise in the temperature-dependent attraction among proteins has been accounted by this potential.

The protein gels are analyzed using two-stage model, usually employed for polymer gel systems (Shibayama, 2012; Valencia et al., 2020). In accordance with this model, we consider mass fractal kind of gel morphology along with presence of large inhomogeneities. To account for the mass fractal morphology of gel network, we have used a Fisher-Burford form factor. In such case, scattering intensity can be represented as (Fisher & Burford, 1967):

$$I(Q) = \left(1 + \frac{2}{3D_f}Q^2R_g^2\right)^{-D_f/2} \tag{6}$$

where D_f is the fractal dimension, R_g is the radius of gyration of the aggregate. The scattering contribution from large inhomogeneities, can be accounted by a power law behavior and equation (6) is modified as:

$$I(Q) = \left(1 + \frac{2}{3D_f}Q^2R_g^2\right)^{-D_f/2} + \frac{I_1}{Q^{-n}} \tag{7}$$

where I_1 is a Q independent proportionality constant, and n denotes the Porod exponent. Since no low Q-cut off is observed in the measured Q range, the consideration of only power law behavior is reasonably acceptable assumption.

The SANS data analysis has been performed by fitting the experimental data to the scattering, calculated from theoretical models and the parameters have been optimized using nonlinear least squares fitting methods (Wignall & Bates, 1987).

3. Results and discussion

3.1. Transmission measurement

Fig. 1a shows the optical transmission of 4 wt% protein dispersion in mixed water/ethanol solvent with increasing temperature. All the transmission values are normalized by the transmission of the 4 wt% BSA solution in water at 25 °C. The transmission of pure BSA decreases systematically with increasing temperature. The decrease in the transmission is usually due to the formation of larger structures in the system, which scatter light more strongly than smaller structures. Therefore, the observed decrease in the transmission can be associated with the protein gelation, which originates due to the unfolding of protein and subsequent protein aggregation, leading to the formation of a 3-dimesional network structure. The transmission of the sample decays faster in the presence of alcohol even at relatively lower temperatures. This suggests that the presence of alcohol promotes the gelation of protein dispersions at a much lower temperature, indicating the cold gelation of the protein. It should be mentioned that neither the pH nor the ionic strength of the sample have been changed which are usually employed to achieve cold gelation for proteins. Fig. 1c shows the gelation temperature variation of the 4 wt% protein dispersion in mixed water/ethanol solvent. As the ethanol concentration was increased, gelation temperature systematically decreased. With 30 % ethanol in solution, the gelation temperature is approximately 37 °C. It should be mentioned that all data in Fig. 1 are based on at least five independent measurements, with the plots showing mean values and appropriate error bars representing standard deviations. The trends were consistent across replicates, supporting the reproducibility and reliability of the results. To further validate the trends, we performed a linear regression analysis on the data presented in Fig. 1C, which shows the variation in gelation temperature as a function of alcohol concentration, a central result of the study. The regression yielded a slope of approximately −1.1, indicating that gelation temperature decreases by about 1.1 °C for each wt.% increase in alcohol concentration. The regression yielded a p-value of ~0.001, confirming that the observed trend is statistically significant ($p < 0.05$). This strongly supports our conclusion that ethanol concentration has a significant and systematic influence on the gelation behavior of BSA.

Interestingly, the effect of alcohol is substantially suppressed with an addition of the anionic surfactant SDS (Fig. 1b). 4 wt% BSA +40 mM SDS prepared in 80/20 water/ethanol solvent does not show any decrease in the transmission and the sample remains in the solution state throughout the measured temperature range. Fig. 1d shows the inversion test of the 4 wt% BSA in 100 % water and in 80/20 water/ethanol mixture, heated at temperatures which are equal or higher to their respective T_G. 4 wt% BSA +40 mM SDS, prepared in 80/20 water/ethanol mixture and heated till 70 °C has also been depicted in the same figure. The system does not show any trace of gelation even at temperatures higher than T_G (~55 °C) of the same sample without SDS (i.e., 4 wt% BSA + 80/20 water/ethanol). To understand these intriguing observations, we have carried out systematic DLS, rheology, and SANS measurements.

3.2. Cold gelation of BSA at different alcohol contents

3.2.1. Size evolution by dynamic light scattering (DLS)

DLS measurements were carried out mostly in the pre-gelation temperatures, as we are aiming to observe the size evolution in the system obtained only from the homodyne component of the intensity auto-correlation function (ACF) (Balakrishnan et al., 2011; Shibayama & Norisuye, 2002). Above the gelation temperature, the heterodyne component in the ACF appears and the data cannot be evaluated using the cumulant analysis method. Therefore, we have investigated the post-gelation temperature region extensively using rheology and SANS. Fig. 2 shows the ACFs of 4 wt% BSA solution in (a) 100 % water and (b) 80/20 (%w/w) water/ethanol mixture with increasing temperature. The

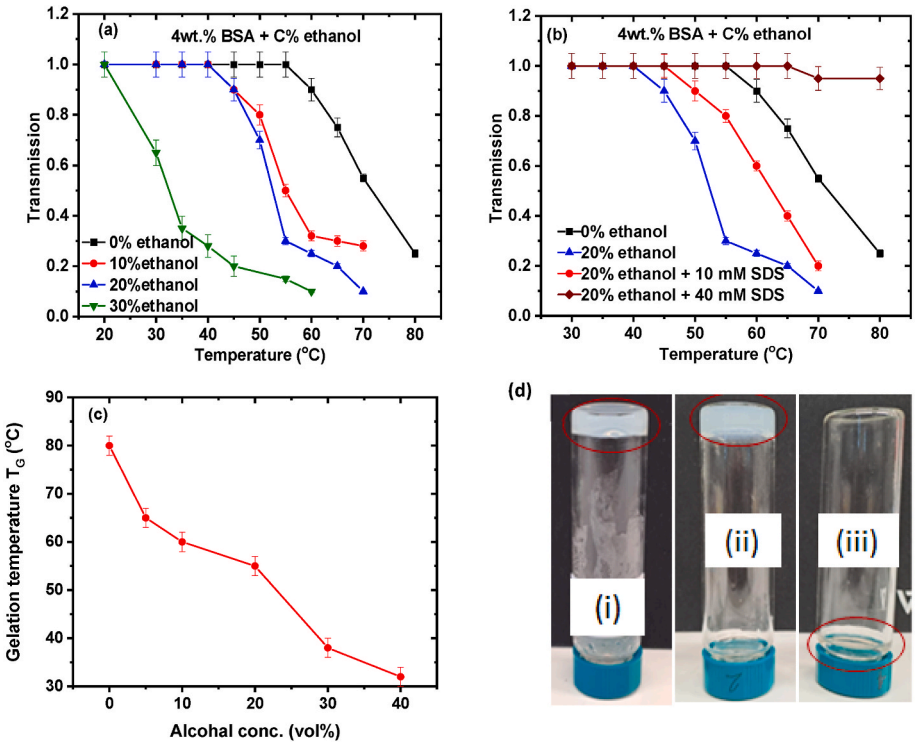

Fig. 1. Transmission of (a) 4 wt% BSA dispersion in mixed water/ethanol solvent with increasing temperature and (b) 4 wt% BSA + 10/40 mM SDS in 80/20 mixed water/ethanol solvent. (c) Gelation temperature (T_G) of 4 wt% BSA in mixed water/ethanol solvent as a function of ethanol concentration. (d) Physical states of the 4 wt% BSA in (i) 100 % water heated at T_G (80 °C), (ii) 80/20 water/ethanol solvent heated at 70 °C and (iii) 4 wt% BSA + 40 mM SDS sample in 80/20 mixed water/ethanol solvent heated at 70 °C.

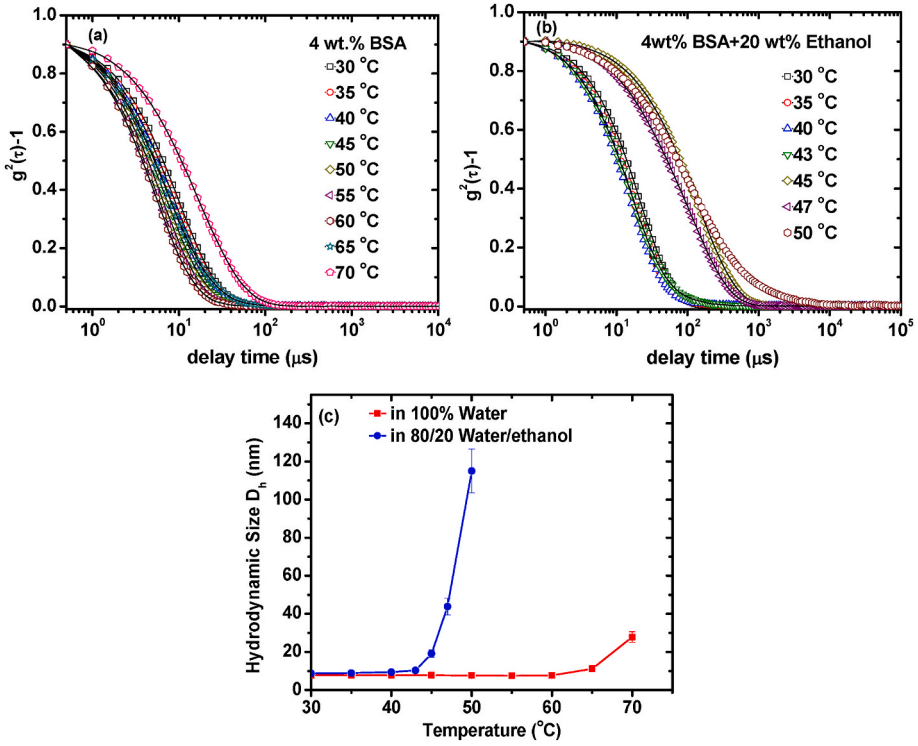

Fig. 2. The intensity autocorrelation functions of 4 wt% BSA solution in (a) 100 % water and (b) 80/20 water/ethanol mixture with increasing temperature, as measured by DLS, and (c) variation of effective hydrodynamic size of the system with increasing temperature as obtained using cumulant analysis.

ACF of the protein.

Solution in water shows a single exponential decay due to monodispersed nature of the protein. As the temperature increases, the ACFs shift towards smaller delay times up to 60 °C. Such shift is attributed to the faster diffusion of protein molecules with an increase in the temperature. The cumulant analysis of the data shows only a marginal increase in the effective hydrodynamic size (D_h) in this temperature range (20–60 °C) [Fig. 2c], which could come from the minor unfolding of the protein molecules. As the temperature increases beyond 60 °C, ACFs shift towards longer delay times, suggesting significant increase in the D_h of the system. Such significant changes in the size of the protein might come from the enhanced hydrophobic attraction or protein network structure formation at higher temperatures (>60 °C). The details of the intermolecular interaction and structure formation of BSA protein under these solvent conditions have been investigated by SANS.

In Fig. 2b, the ACFs show only a marginal shift towards lower delay times up to a temperature of 43 °C, mostly due to temperature-driven enhancement in protein diffusion. ACFs shift significantly towards longer delay times for further increase in the temperature. A significant rise in the effective hydrodynamic size was observed at a temperature as low as 50 °C. This is in an agreement with the transmission measurement (Fig. 1), which suggests that the presence of ethanol accelerates the gel formation of BSA protein. Moreover, an increase in the D_h at much lower temperatures could be attributed to the alcohol-assisted protein unfolding and thereby enhancing hydrophobic attraction even at lower temperatures (Malkin et al., 2023; Singh et al., 2010). The circular dichroism results also show that ethanol induces a significant loss in the α-helical content of BSA even at room temperature, confirming partial unfolding of the protein structure [Fig. S1 and Table S1 in supplementary information (SI)], supporting our inferences that ethanol facilitates cold gelation by destabilizing the native protein conformation. This observation is consistent with literature reports, which suggest that The interplay of entropy and enthalpic interactions could cause the nonspecific alcohol binding, where a large number of alcohol molecules penetrates into the hydrophobic interior of protein, leading to loss of native protein structure (Chong et al., 2015).

DLS data of 4 wt% BSA solutions, prepared in 95/5 and 90/10 water/ethanol mixed solvents with increasing temperature are depicted in Fig. S2 and S3 in SI. Like the results observed for 20 wt% ethanol, the data show similar trend at lower ethanol contents. Overall, the propensity of increasing the effective hydrodynamic size of BSA protein is enhanced with increasing ethanol content in the solution (Figs. 1 and 2, S2, and S3).

3.2.2. *Rheological behavior of the gel*

The rheological characteristics of the gel have been studied by carrying out frequency sweep measurements. Fig. 3 shows the variation in the storage (G') and loss (G'') modulus of gels prepared on heating the 4

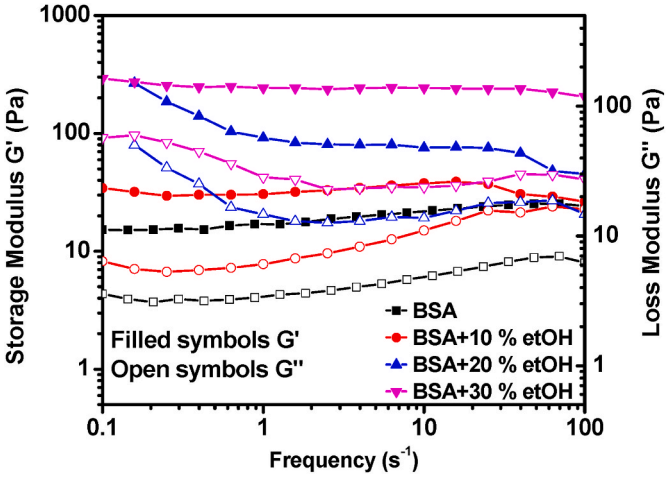

Fig. 3. Measured rheology data (storage (G') and loss (G'') moduli) of the BSA gels prepared in different water/ethanol mixtures, with varying ethanol concentration.

wt% BSA dispersion in the mixed water/ethanol with varying ethanol concentrations. The gel samples, prepared by heating the solutions in closed vials at respective gelation temperatures, were placed in the rheometer and the measurements carried.

Out at room temperature. The storage modulus (G') of BSA gel remain more or less constant and more than loss modulus (G'') throughout the measured frequency range, satisfying the required condition for gel formation (Malkin et al., 2023). The trend in the variation of G' and G'' remain the same with an addition of ethanol, representing the typical characteristics of the gel. However, the storage modulus increases significantly with increasing ethanol content, suggesting that the gel strength is increasing with increasing ethanol fraction in the solvent (Andreadis & Moschakis, 2023a). In fact, the slope of variation of G' does not vary significantly with respect to frequency in case of 4 wt% BSA sample, prepared in 70/30 water/ethanol mixture, indicating purely elastic nature of the gel (Xi et al., 2019).

3.2.3. *Evolution of structure studied by SANS: effect of ethanol content*

The evolution of interaction in protein from pristine state to the gel formation and the resultant morphology of the gels have been probed by SANS. Fig. 4a shows the SANS data of 4 wt% BSA dispersion with an increase in the temperature from 20 °C to 65 °C. Data of BSA at 20 °C mostly shows a monotonically decreasing profile, suggesting only $P(Q)$ governed.

scattering, and hence $S(Q)$ is approximated to unity. Therefore, the scattering data were fitted using a $P(Q)$, corresponding to an oblate ellipsoidal shape, which captures the overall geometry of the protein molecules. The fitted parameters are consistent with the dimensions of BSA reported in the literature (Zhang et al., 2012). The data shows a systematic build-up of the scattering intensity in the low Q-region on increasing the temperature up to 65 °C. The systematic rise in the scattering intensity usually exhibits an evolution of the attractive interaction in the system or the formation of larger structures. Since the data in the higher Q region ($Q > 0.05$ Å^{-1}) remains more or less same, the formation of larger aggregates can be ruled out. Therefore, the data are fitted considering $P(Q)$ of oblate ellipsoidal shape with $S(Q)$ of short-range attractive square-well potential (Bharti et al., 2014; Corbett et al., 2017; Kumar et al., 2024). Fitted parameters are listed in Table 1. On increasing temperature, the protein molecules show a systematic increase in the geometrical parameters, consistent with slight unfolding of the protein. In addition, the system shows a significant rise in attractive interaction, as reflected from the increased depth and range of the fitted square-well potential (Table 1). The rise in the attraction with temperature can be mostly attributed to the exposure of the hydrophobic segments towards the aqueous environment. The depth potential is found to be more than average thermal kinetic energy ($1.5k_BT$) of the molecules, while the range is also more than equivalent diameter [$2(a^2b)^{1/3}$] of the protein. Both of these parameters suggest that strong attraction acting over longer distances to finally causing protein gelation at T_G (Flores-Tandy et al., 2020).

The tendency of gelation of BSA protein is substantially enhanced in the presence of ethanol. Fig. 4b–d shows the SANS data of 4 wt% BSA in 95/5, 90/10 and 80/20 mixed D_2O/ethanol solvent, respectively. One can observe that the signal-to-background ratio of 4 wt% BSA at 30 °C systematically reduces with increasing ethanol content. This is mostly due to an increase in the incoherent background, originating from the hydrogen present in ethanol and significant decrease in the scattering contrast between protein and mixed solvent. Comparison of the SANS data of BSA in 100 % D_2O and mixed D_2O/ethanol systems at 30 °C show a slight modification in the BSA dimensions in the presence of alcohol, consistent with the alcohol driven changes in the secondary structure of

Table 1
Fitted parameters of SANS data of 4 wt% BSA solution prepared in 100 % D_2O.

Temperature (°C)	Semi-major axis $a = c$ (nm)	Semi-minor axis b (nm)	Depth of potential (k_BT)	Width of potential (nm)
30	4.3 ± 0.2	1.4 ± 0.1	–	–
50	4.3 ± 0.2	1.4 ± 0.1	–	–
60	4.5 ± 0.2	1.5 ± 0.1	5.2 ± 0.3	3.7 ± 0.2
65	4.6 ± 0.2	1.5 ± 0.1	8.0 ± 0.4	4.8 ± 0.3

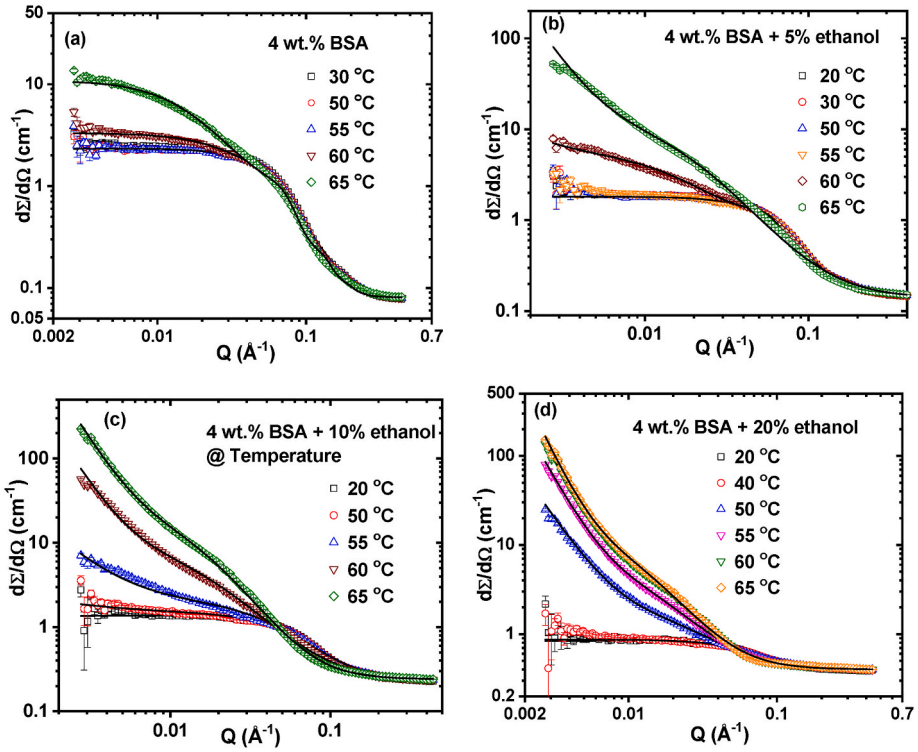

Fig. 4. SANS data of 4 wt% BSA in (a) 100 % D_2O, (b) 95/5, (c) 90/10 and (d) 80/20 ratio of D_2O/ethanol mixed solvent with increasing temperature.

the protein (Dirauf et al., 2021).

The scattering data of 4 wt% BSA in 95/05 mixed D_2O/ethanol (Fig. 4b) do not show any significant changes up to 55 °C. However, the further increase in the temperature leads to significant changes in the scattering profile as can be seen from the upturn of the scattering intensity in the lower-Q regime (Fig. 4b). As the alcohol content in the system is increased, the low-Q rise in scattering intensity is noted to be appearing at lower temperatures (Fig. 4b–d). For example, the data in the presence of 5 %, 10 %, and 20 % ethanol show an increase in scattering intensity at 60, 55, and 50 °C, respectively. Above these respective temperatures, each system shows clear indications of gel formation in the scattering profile (discussed later). In the case of 20 % ethanol (Fig. 4d), the signature of gel formation in data is evident at temperatures as low as 50 °C. The scattering signal overlaps at 60 and 65 °C, suggesting that the gel formation is almost complete at these temperatures and no further structural modifications are expected beyond this temperature range (>65 °C). It is thus clear that the increase in ethanol content reduces the gelation temperature and accelerates the gel formation at much lower temperatures (cold-set gelation). The SANS results are quite consistent with the transmission and DLS data (Figs. 1 and 2) where decrease in gelation temperature and significant rise in effective hydrodynamic size are also observed with increasing ethanol content.

The rise in the scattering intensity with increasing temperature shows in Fig. 4b–d is not similar to that observed Fig. 4a, where the system was only undergoing attractive interaction. In fact, in later cases (Fig. 4b–d), the low-Q rise in the scattering intensity is accompanied by linearity in the scattering profile along with substantial changes in the intermediate Q values, suggesting the formation of hierarchical fractal structure in the system. At higher temperatures, the scattering profile shows features of two length scales, as can be clearly noticed in Fig. 4d, where the slope of the linearity shows change at Q ~0.007 $Å^{-1}$. The scattering signal in the Q region >0.007 $Å^{-1}$ is accounted by the fractal morphology of the resulting gel, whereas data in the very low Q range ($Q < 0.007$ $Å^{-1}$) is attributed to the presence of large inhomogeneities in the gels (equation (7)). Accordingly, the data are fitted using two-stage model of the polymer gels (Parsana et al., 2023; Shibayama, 2012). This model considers two contributions: (i) the gel network as a fractal structure, which is appropriate for the hierarchical and percolated nature of the protein gels, and (ii) the presence of large-scale inhomogeneities. Fractal morphology of the gels is taken care by Fisher-Burford model, considering exponential cut-off function, as described in section 2.3.2 (Ferri et al., 2001; John et al., 2019; Österberg & Mortensen, 1994). The fractal dimension describes the compactness of the gel network, while the radius of gyration reflects the overall size of the mass fractals. The fitted parameters are listed in Table 2. Both parameters show a systematic increase with temperature for all the alcohol contents, suggesting the formation of more compact and large protein network. For temperatures more than T_G at respective ethanol contents, the Porod exponent is noted to be higher than 3, suggesting presence of highly compact larger inhomogeneities with surface fractal kind of morphologies. These large inhomogeneities could represent certain regions of highly compact and dense cross-linking of unfolded protein in the gel network (Shibayama, 2012, 2025). As the temperature increases the value of exponent further increases, suggesting shrinkage (enhancement in the compactness) of these regions. A comparison of the radius of gyration, Porod exponent, and the fractal dimension with the change in the ethanol fraction (Table 2) shows that the cross linking or networking in the resulting gels also increases with an increasing alcohol concentration at a given temperature, thereby giving rise to higher strength to the gel, as also observed in rheology data (Fig. 3).

3.2.4. SANS evidence of cold gelation of BSA protein at room temperature

It has been seen in Fig. 1 that the gelation of BSA can be achieved close to the room temperature by increasing the ethanol content beyond 30 %. This is also evident from SANS results in Fig. 5, which compares

Table 2

(a) Fitted parameters of SANS data of 4 wt% BSA solution prepared in 95/5 ratio of D_2O/ethanol mixed solvent.

Temperature (oC)	Semi-major axis a = c (nm)	Semi-minor axis b (nm)	
20	4.2 ± 0.2	1.4 ± 0.1	
30	4.2 ± 0.2	1.4 ± 0.1	
50	4.2 ± 0.2	1.4 ± 0.1	
55	4.2 ± 0.2	1.4 ± 0.1	
Initiation of gel formation			
Temperature (°C)	**Radius of gyration R_g (nm)**	**Fractal dimension (D_f)**	**Porod exponents (n_1)**
60	8.2 ± 1.0	2.0 ± 0.1	–
65	10.5 ± 1.0	2.15 ± 0.1	2.7 ± 0.1

(b) Fitted parameters of SANS data of 4 wt% BSA solution prepared in 90/10 ratio of D_2O/ethanol mixed solvent.

Temperature (°C)	Semi-major axis a = c (nm)	Semi-minor axis b (nm)	
20	3.8 ± 0.2	1.2 ± 0.1	
50	4.4 ± 0.2	1.4 ± 0.1	
Initiation of gel formation			
Temperature (°C)	**Radius of gyration R_g (nm)**	**Fractal dimension (D_f)**	**Porad exponents (n_1)**
55	6.2 ± 0.5	2.0 ± 0.1	–
60	11.0 ± 1.0	2.0 ± 0.1	3.0 ± 0.1
65	13.2 ± 1.0	2.7 ± 0.1	3.1 ± 0.1

(c) Fitted parameters of SANS data of 4 wt% BSA solution prepared in 80/20 ratio of D_2O/ethanol mixed solvent.

Temperature (°C)	Semi-major axis a = c (nm)	Semi-minor axis b (nm)	
20	3.6 ± 0.2	1.2 ± 0.1	
40	3.6 ± 0.2	1.2 ± 0.1	
Initiation of gel formation			
Temperature (°C)	**Radius of gyration R_g (nm)**	**Fractal dimension (D_f)**	**Porod exponents (n_1)**
50	6.2 ± 0.5	2.0 ± 0.1	2.5 ± 0.1
55	11.4 ± 1.0	2.1 ± 0.1	3.1 ± 0.1
60	13.4 ± 1.0	2.4 ± 0.1	3.4 ± 0.1
65	13.5 ± 1.0	2.5 ± 0.1	3.5 ± 0.1

the SANS data of 4 wt% BSA in pure D_2O and D_2O with increasing ethanol content, measured at 30 °C and 65 °C. At 30 °C, BSA prepared in 70/30 D_2O/ethanol solvent show signatures of gel formation, whereas rest of the data show features of scattering from BSA molecules in solution state (Fig. 5a). Systematic decrease in the scattering signal and rise in the background (high Q-region) up to alcohol content of 20 % can be attributed to the alcohol enhancing the incoherent background and decreasing the contrast of BSA molecules in mix ethanol/D_2O solvents compared to pure D_2O, as discussed earlier. However, as the alcohol content is increased to 30 %, the scattering intensity shows sharp linear scattering in the low Q-region, as typically observed on gel formation, confirming the room temperature gelation of protein at 30 % ethanol content. SANS data of BSA in 70/30 D_2O/ethanol solvent with systematic temperature change are depicted in Fig. S4 in SI. The scattering profiles overlap at temperatures more than 40 °C, suggesting saturation of modifications in structural features of gel at temperatures as low as 40 °C (Fig. S4 in SI).

All the data at 65 °C in Fig. 5b show the signature of gel formation except that of the pure BSA protein, where the protein molecules still undergo attractive interaction (Table 1). Apart from a rise in scattering intensity in high Q-region, as originating from high incoherent background (discussed above), the data sets in Fig. 5b also show an increase in the scattering intensity particularly in the low Q-region ($Q < 0.01$ $Å^{-1}$) with an addition of alcohol, due to the formation of networking structure of protein gels. The fitting of these data sets using two-stage model are described earlier and the fitted parameters are present in Table 2. Interestingly at 30 wt% alcohol content, the data show large linear scattering with a power law dependence of about Q^{-3} in the

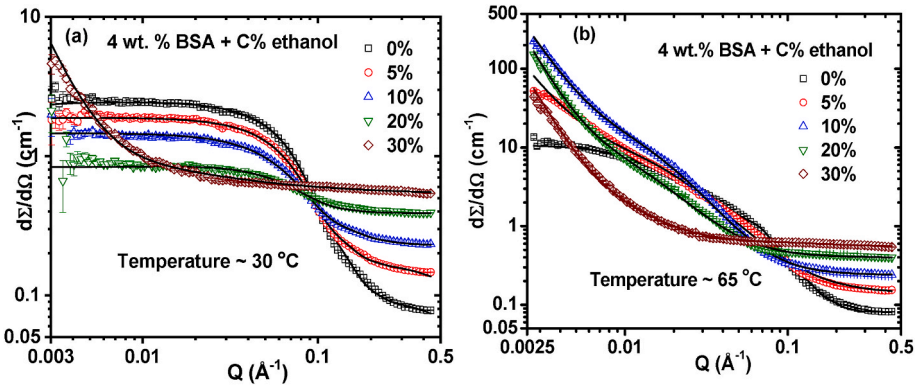

Fig. 5. SANS data of 4 wt% BSA in mixed D_2O/ethanol solvent with varying fraction of ethanol measured at (a) 30 °C and (b) 65 °C.

almost entire *Q*-range (0.003–0.01 $Å^{-1}$), with almost no broad humplike scattering features in the intermediate *Q*-range (0.01–0.05 $Å^{-1}$), as observed in the case of lower alcohol contents. The absence of intermediate scattering features may originate from the collapse of the intermediate mass fractal kind of network structure and the formation of quite compact agglomerated structure of the protein gel, at this alcohol concentration (30 wt%). This is consistent with scanning electron microscopy images (Fig. S5) as well as our rheology data, showing the formation of highest strength gels at this alcohol concentration.

3.3. Inhibition of cold gelation of BSA protein

The data discussed so far provides details on evolution of structures of alcohol-driven cold gelation of BSA protein solution. Intriguingly, such a tendency of the protein solution to undergo cold-set gel in water/ethanol mixed solvent can be suppressed by adding the anionic surfactant, SDS, to the system. This is demonstrated by measuring the gelation temperature of the BSA solutions in presence of varying contents of ethanol and SDS (Table S2 in SI). The measurements demonstrate that while ethanol consistently reduces the gelation temperature, SDS tends to counteract this effect by increasing the gelation temperature and, at sufficiently high concentrations, can even prevent gelation altogether. Fig. 6a shows ACFs of 4 wt% BSA in 90/10 water/ethanol mixture in presence of 40 mM SDS. The result exhibits that unlike pure BSA suspensions in water as well as water/ethanol mixtures (Fig. 2) there is almost no shift in the ACFs towards longer delay times with increasing temperature. Instead, there is a slight shift in the ACF towards shorter delay time at 70 °C, mostly due to the faster diffusion of the scatterers at higher temperature (protein molecules and SDS micelles in this case). Fig. 6c shows the variation of the effective hydrodynamic size of 4 wt% BSA with 40 mM SDS in 10 % and 20 % ethanol/water mixtures with increasing temperature, which depicts no substantial increase in the size of scatterers. Each data point in this figure represents the mean value of five independent measurements, with standard deviation as error bars. We performed linear regression analysis for both datasets. The obtained slopes were 0.07 (for 10 % ethanol) and 0.02 (for 20 % ethanol), with

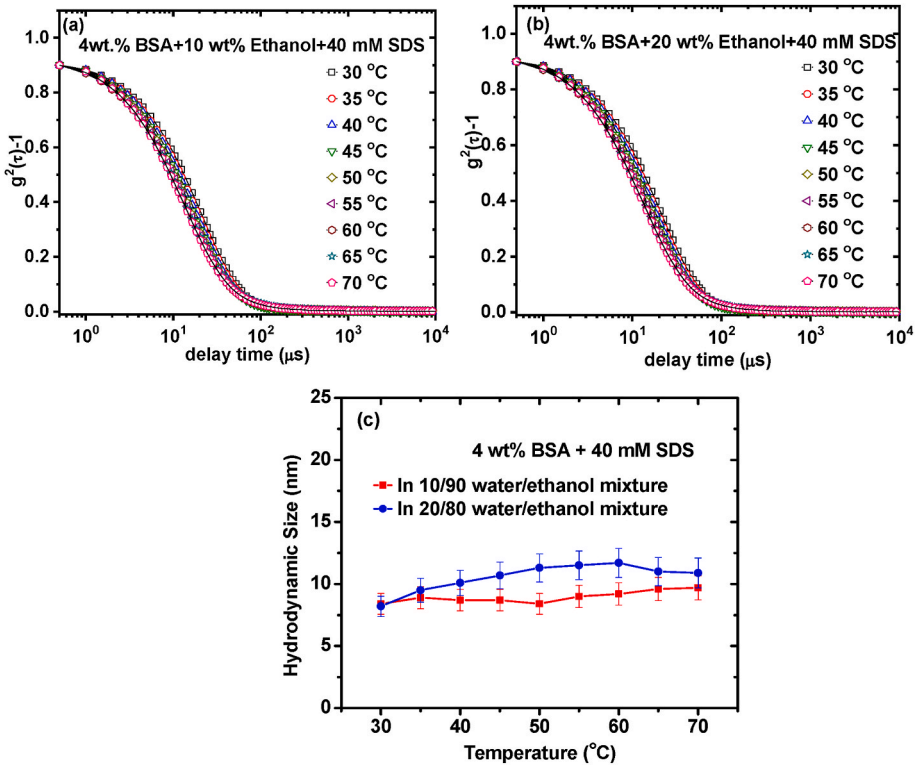

Fig. 6. ACFs of 4 wt% BSA +40 mm SDS solutions in (a) 10 % ethanol and (b) 20 % ethanol in mixed ethanol/water solvents with increasing temperature, as measured by dynamic light scattering. (c) Effective hydrodynamic size of the systems as obtained by DLS.

corresponding p-values of 0.005 and 0.007. While statistically significant, the slopes are numerically small, indicating that temperature has only a marginal effect on hydrodynamic size.

The ionic micelles (e.g., SDS or DTAB) are known to display a marginal scaling down in the size with increasing temperature. On the other hand, protein molecules should show an increase in the size, if it is undergoing temperature-driven unfolding and subsequent gelation. Since the DLS data are usually dominated by the larger structures, no significant increase in the effective hydrodynamic size of the system suggests no substantial change in protein dimensions, clearly restricting the protein gelation (Kumar & Aswal, 2024; Kumar et al., 2023).

Similar effects were observed for 4 wt% BSA in 80/20 water/ethanol mixture in presence of 40 mM SDS (Fig. 6b). The ACFs of this system also do not shift towards longer delay times even at higher temperatures and there is almost no change in hydrodynamic size (Fig. 6c). The role of SDS here may appear counter-intuitive as it is known to unfold the protein as applied in gel electrophoresis. In some cases, SDS is also reported to provide protective effects against temperature driven protein denaturation and gelation (Moriyama et al., 2008; O. S. Nnyigide & Hyun, 2020; Xu & Keiderling, 2004). In fact, even in the absence of ethanol, the BSA + SDS solutions (prepared in 100 % water) do not show significant rise in hydrodynamic sizes with increasing temperature (Fig. S6 in SI). In agreement to the protective effect of SDS, the above DLS results also demonstrate the ability of SDS to suppress the alcohol-induced cold-set gelation of the BSA protein.

To understand the role of SDS in suppressing the ethanol-induced protein gelation, we carried out SANS measurements of 4 wt% BSA prepared in 80/20 D_2O/ethanol mixture with 10 and 40 mM SDS at 55 °C (Fig. 7). For comparison, SANS data of 4 wt% BSA in mixed solvent measured at 55 °C is also shown in Fig. 7. At this temperature, the BSA protein in mixed solvent undergoes immediate gelation in absence of SDS as discussed in Fig. 1c and 4d. The features of the scattering data of 4 wt% BSA in presence of SDS at 55 °C are different from that of the BSA in mixed solvent. In fact, the features of the data of 4 wt% BSA with 40 mM SDS at 55 °C resemble those of the pure BSA solution as discussed in Fig. 4a. However, data of 4 wt% BSA with10 mM SDS shows higher scattering in the low-Q region compared to that for 40 mM SDS, suggesting that effect of SDS in suppressing the gelation is less significant at lower SDS concentration. The scattering intensity in presence of SDS at 55 °C could be fitted by considering the protein molecules undergoing attractive interaction (no gelation) along with the contribution from pure SDS micelles. The fitted parameters are given in Table 3. One can

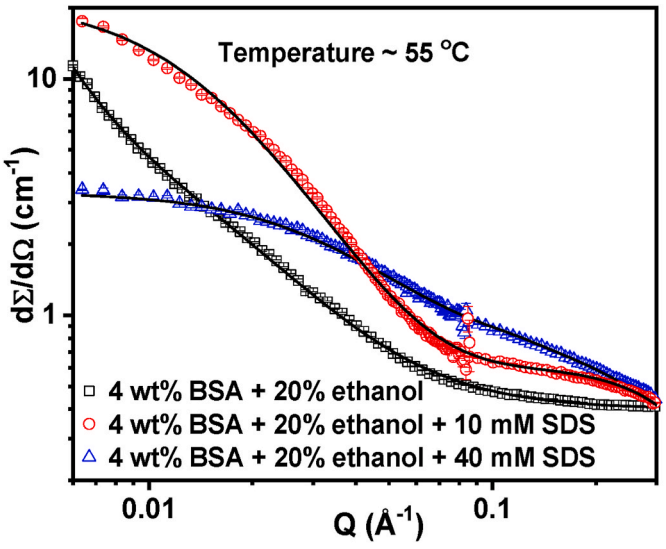

Fig. 7. SANS data of 4 wt% BSA without and with 10 and 40 mM SDS, prepared 80/20 water/ethanol mix solvent.

Table 3
Fitted parameters of SANS data of 4 wt% BSA with C mM SDS solution prepared in 20 % ethanol/D_2O. The contribution of small spherical micelles (mean radius ~ 2.0 nm) of SDS has also been considered.

SDS Conc. (mM)	Semi-major axis $a = c$ (nm)	Semi-minor axis b (nm)	Depth of potential (k_BT)	Width of potential (nm)
10	5.0	1.5	10	4.5
40	4.6	1.4	7	3.1

note in Table 3 that the attraction among protein molecules (depth/width of potential) is decreasing with increasing SDS concentration. This is consistent with the transmission plot (Fig. 1b), where the 4 wt% BSA with 10 mM SDS in 20 % ethanol/water mixture is seen undergoing gelation at 65 °C, while 4 wt% BSA with 40 mM SDS in mixed solvent does not show any gelation even up to 70 °C. SANS data of 4 wt% BSA protein prepared in mixed solvent and contains different amount of SDS (0–40 mM), measured at 65 °C are shown in Fig. S7 in SI. The data at lower concentrations of SDS ($C_{SDS} \leq 20$ mM) show the signature of gel formation, whereas with 40 mM SDS, the system remains in the solution state. Thus, our results suggest that the complete inhibition of gelation and/or tuning of gelation temperature depends on the relative amount of SDS and ethanol.

The observed effect of SDS in preventing/delaying the gel formation of the BSA protein in the presence of ethanol could be due to either (i) suppression of hydrophobic attraction and/or (ii) enhancement in the electrostatic repulsion in the system. Both factors tend to suppress the gel formation tendency in the protein solutions on heating by making the system's overall behavior less attractive (Table 3). It has been observed that alcohol interacts with SDS micelles either at the water/head-group interface or inside the micelle core (Méndez-Bermúdez & Dominguez, 2016), which may in part explain the reduced effect of alcohol on BSA. Also, another factor is anionic SDS micelles will enhance the overall charge-charge interaction in the system (Kumar & Aswal, 2024). SDS, being an anionic surfactant, can bind only to the positively charged patches on the negatively charged BSA molecule. This binding leads to an overall increase in the net negative charge, which in turn enhances electrostatic repulsion between protein molecules. This is confirmed by zeta potential and SANS measurements in our previous study (Kumar & Aswal, 2024). This electrostatic stabilization likely prevents the aggregation and network formation necessary for gelation, even in the presence of ethanol. Additionally, prior studies have shown that the addition of salt (NaCl) can enhance SDS-induced unfolding by screening repulsive interactions (Mehan et al., 2015; Saha et al., 2018), further supporting our mechanistic interpretation. Others have also reported such protective effect of SDS against thermal denaturation/gelation of BSA (in the absence of ethanol) [Kumar & Aswal, 2024; Kumar et al., 2025; T. O. Nnyigide et al., 2023], as mentioned above. They attributed these effects to enhanced electrostatic repulsion as well as reduction in hydrophobic attraction due to the formation of favorable hydrogen bonds between the protein and SDS and the formation of cross-linking bridges. Therefore, the inhibition of ethanol-induced BSA gel formation by SDS can be defined as the interplay of hydrophobic attraction and electrostatic repulsion in the system.

The ability to tune gelation temperature down to near-room temperature through ethanol offers a controlled, low-energy pathway for structuring proteins with an advantage in applications where thermal sensitivity is critical, such as in food processing and biomedical formulations. Furthermore, the demonstration that SDS can inhibit this gelation through modulation of electrostatic and hydrophobic interactions adds a new layer of control in protein structuring strategies. These insights may aid in the rational design of soft protein-based materials with tailored textures and mechanical properties.

4. Conclusions

This study demonstrates that ethanol can effectively induce cold-set gelation of BSA protein at temperatures as low as room temperature. The strength of the resulting gel is also enhanced by increasing the ethanol content. The addition of the anionic surfactant, sodium dodecyl sulfate (SDS), prevents gelation even under conditions that would otherwise promote it. This inhibition underscores the role of surfactants in modulating protein interactions. The findings analyzed using SANS, DLS, and rheology, reveal that the gelation process is significantly influenced by the interplay between alcohol, temperature, and surfactants, offering insights relevant to applications in biomedicine and the food industry.

CRediT authorship contribution statement

Debasish Saha: Writing – original draft, Validation, Supervision, Methodology, Investigation, Funding acquisition, Formal analysis, Data curation, Conceptualization. **Sugam Kumar:** Writing – original draft, Validation, Supervision, Methodology, Investigation, Formal analysis, Data curation, Conceptualization. **Purushottam S. Dubey:** Writing – review & editing, Methodology. **Jitendra P. Mata:** Writing – review & editing, Methodology. **Andrew E. Whitten:** Writing – review & editing, Methodology. **Joachim Kohlbrecher:** Writing – review & editing, Resources, Methodology. **Henrich Frielinghaus:** Writing – review & editing, Methodology, Investigation, Funding acquisition. **Vinod K. Aswal:** Writing – review & editing, Validation, Methodology, Investigation.

Declaration of competing interest

The authors declare no competing financial interest.

Acknowledgements

D.S. wishes to thank Forschungszentrum Juelich (FZJ), Germany and GNeuS (Global Neutron Scientist) fellowship, co-funded by Marie Skłodowska-Curie Grant Agreement N°101034266. D.S. also thank Australian Nuclear Science and Technology Organization (ANSTO), Australia and Paul Scherrer Institute (PSI), Switzerland for providing the beam time (Proposal No-P17002, P17256, and 20241329) for SANS experiments.

Appendix A. Supplementary data

Supplementary data to this article can be found online at https://doi.org/10.1016/j.foodhyd.2025.111991.

Data availability

Data will be made available on request.

References

Ako, K., Nicolai, T., & Durand, D. (2010). Salt-induced gelation of globular protein aggregates: Structure and kinetics. *Biomacromolecules, 11*(4), 864–871. https://doi.org/10.1021/bm9011437

Alting, A. C., van der Meulena, E. T., Hugenholtz, J., & Visschers, R. W. (2004a). Control of texture of cold-set gels through programmed bacterial acidification. *International Dairy Journal, 14*(4), 323–329. https://doi.org/10.1016/j.idairyj.2003.09.008

Alting, A. C., Weijers, M., de Hoog, E. H. A., van de Pijpekamp, A. M., Cohen Stuart, M. A., Hamer, R. J., de Kruif, C. G., & Visschers, R. W. (2004b). Acid-induced cold gelation of globular proteins: Effects of protein aggregate characteristics and disulfide bonding on rheological properties. *Journal of Agricultural and Food Chemistry, 52*(3), 623–631. https://doi.org/10.1021/jf034753r

Andlinger, D. J., Schlemmer, L., Jung, I., Schroeter, B., Smirnova, I., & Kulozik, U. (2022). Hydro- and aerogels from ethanolic potato and whey protein solutions: Influence of temperature and ethanol concentration on viscoelastic properties, protein interactions, and microstructure. *Food Hydrocolloids, 125*, Article 107424. https://doi.org/10.1016/j.foodhyd.2021.107424

Andreadis, M., & Moschakis, T. (2023). Formation of thermo-reversible gels from whey proteins after combined thermal and ethanol pretreatment. *Food Hydrocolloids, 142*, Article 108749. https://doi.org/10.1016/j.foodhyd.2023.108749

Andreadis, M., & Moschakis, T. (2023a). Effect of ethanol on gelation and microstructure of whey protein gels in the presence of NaCl. *Food Hydrocolloids, 134*, Article 107985. https://doi.org/10.1016/j.foodhyd.2022.107985

Arabi, S. H., Haselberger, D., & Hinderberger, D. (2020). The effect of ethanol on gelation, nanoscopic, and macroscopic properties of serum albumin hydrogels. *Molecules, 25*(8), 1927. https://doi.org/10.3390/molecules25081927

Arnold, O., Bilheux, J. C., Borreguero, J. M., Buts, A., Campbell, S. I., Chapon, L., Doucet, M., Draper, N., Ferraz Leal, R., Gigg, M. A., Lynch, V. E., Markvardsen, A., Mikkelson, D. J., Mikkelson, R. L., Miller, R., Palmen, K., Parker, P., Passos, G., Perring, T. G., … Zikovsky, J. (2014). Mantid—data analysis and visualization package for neutron scattering and μ SR experiments. *Nuclear Instruments and Methods in Physics Research Section A: Accelerators, Spectrometers, Detectors and Associated Equipment, 764*, 156–166. https://doi.org/10.1016/j.nima.2014.07.029

Balakrishnan, G., Durand, D., & Nicolai, T. (2011). Particle diffusion in globular protein gels in relation to the gel structure. *Biomacromolecules, 12*(2), 450–456. https://doi.org/10.1021/bm101238r

Banc, A., Charbonneau, C., Dahesh, M., Appavou, M.-S., Fu, Z., Morel, M.-H., & Ramos, L. (2016). Small angle neutron scattering contrast variation reveals heterogeneities of interactions in protein gels. *Soft Matter, 12*(24), 5340–5352. https://doi.org/10.1039/C6SM00710D

Bayrak, M., Mata, J., Conn, C., Floury, J., & Logan, A. (2023). Application of small angle scattering (SAS) in structural characterisation of casein and casein-based products during digestion. *Food Research International, 169*, Article 112810. https://doi.org/10.1016/j.foodres.2023.112810

Bharti, B., Meissner, J., Klapp, S. H. L., & Findenegg, G. H. (2014). Bridging interactions of proteins with silica nanoparticles: The influence of pH, ionic strength and protein concentration. *Soft Matter, 10*(5), 718–728. https://doi.org/10.1039/C3SM52401A

Boulet, M., Britten, M., & Lamarche, F. (2001). Dispersion of food proteins in water-alcohol mixed dispersants. *Food Chemistry, 74*(1), 69–74. https://doi.org/10.1016/S0308-8146(01)00099-1

Cao, Y., & Mezzenga, R. (2020). Design principles of food gels. *Nature Food, 1*(2), 106–118. https://doi.org/10.1038/s43016-019-0009-x

Chong, Y., Kleinhammes, A., Tang, P., Xu, Y., & Wu, Y. (2015). Dominant alcohol–protein interaction via hydration-enabled enthalpy-driven binding mechanism. *The Journal of Physical Chemistry B, 119*(17), 5367–5375. https://doi.org/10.1021/acs.jpcb.5b00378

Clark, A. H., Kavanagh, G. M., & Ross-Murphy, S. B. (2001). Globular protein gelation—Theory and experiment. *5th International Hydrocolloids Conference, 15*(4), 383–400. https://doi.org/10.1016/S0268-005X(01)00042-X

Corbett, D., Hebditch, M., Keeling, R., Ke, P., Ekizoglou, S., Sarangapani, P., Pathak, J., Van Der Walle, C. F., Uddin, S., Baldock, C., Avendaño, C., & Curtis, R. A. (2017). Coarse-grained modeling of antibodies from small-angle scattering profiles. *The Journal of Physical Chemistry B, 121*(35), 8276–8290. https://doi.org/10.1021/acs.jpcb.7b04621

Dirauf, M. P., Hajnal, A., Gurikov, P., & Braeuer, A. S. (2021). Protein gel shrinkage during solvent exchange: Quantification of gel compaction, mass transfer and compressive strength. *Food Hydrocolloids, 120*, Article 106916. https://doi.org/10.1016/j.foodhyd.2021.106916

Dubey, P., Kumar, S., Aswal, V. K., Ravindranathan, S., Rajamohanan, P. R., Prabhune, A., & Nisal, A. (2016). Silk fibroin-sophorolipid gelation: Deciphering the underlying mechanism. *Biomacromolecules, 17*(10), 3318–3327. https://doi.org/10.1021/acs.biomac.6b01069

Ferri, F., Greco, M., Arcovito, G., Bassi, F. A., De Spirito, M., Paganini, E., & Rocco, M. (2001). Growth kinetics and structure of fibrin gels. *Physical Review E, 63*(3), Article 031401. https://doi.org/10.1103/PhysRevE.63.031401

Fisher, M. E., & Burford, R. J. (1967). Theory of critical-point scattering and correlations. I. The ising model. *Physical Review, 156*(2), 583–622. https://doi.org/10.1103/PhysRev.156.583

Flores-Tandy, L. M., García-Monjaraz, A. V., van Nierop, E. A., Vázquez-Martínez, E. A., Ruiz-Garcia, J., & Mejía-Rosales, S. (2020). Fractal aggregates formed by ellipsoidal colloidal particles at the air/water interface. *Colloids and Surfaces A: Physicochemical and Engineering Aspects, 590*, Article 124477. https://doi.org/10.1016/j.colsurfa.2020.124477

Gao, X., Yao, Y., Wu, N., Xu, M., Zhao, Y., & Tu, Y. (2020). The sol-gel-sol transformation behavior of egg white proteins induced by alkali. *International Journal of Biological Macromolecules, 155*, 588–597. https://doi.org/10.1016/j.ijbiomac.2020.03.209

Gilbert, E. P. (2023). Neutron techniques for food hydrocolloids. *Current Opinion in Colloid & Interface Science, 67*, Article 101730. https://doi.org/10.1016/j.cocis.2023.101730

Gosal, W. S., & Ross-Murphy, S. B. (2000). Globular protein gelation. *Current Opinion in Colloid & Interface Science, 5*(3), 188–194. https://doi.org/10.1016/S1359-0294(00)00057-1

Jeffries, C. M., Ilavsky, J., Martel, A., Hinrichs, S., Meyer, A., Pedersen, J. S., Sokolova, A. V., & Svergun, D. I. (2021). Small-angle X-ray and neutron scattering. *Nature Reviews Methods Primers, 1*(1), 70. https://doi.org/10.1038/s43586-021-00064-9

John, J., Ray, D., Aswal, V. K., Deshpande, A. P., & Varughese, S. (2019). Dissipation and strain-stiffening behavior of pectin–Ca gels under LAOS. *Soft Matter, 15*(34), 6852–6866. https://doi.org/10.1039/C9SM00709A

Kaewprasit, K., Kobayashi, T., & Damrongsakkul, S. (2018). Thai silk fibroin gelation process enhancing by monohydric and polyhydric alcohols. *International Journal of*

Biological Macromolecules, 118, 1726–1735. https://doi.org/10.1016/j.ijbiomac.2018.07.017
Kaszuba, M., McKnight, D., Connah, M. T., McNeil-Watson, F. K., & Nobbmann, U. (2008). Measuring sub nanometre sizes using dynamic light scattering. *Journal of Nanoparticle Research, 10*(5), 823–829. https://doi.org/10.1007/s11051-007-9317-4
Keiderling, U. (2002). The new 'BerSANS-PC' software for reduction and treatment of small angle neutron scattering data. *Applied Physics A, 74*(1), s1455–s1457. https://doi.org/10.1007/s003390201561
Kumar, S., & Aswal, V. K. (2024). Evolution of the structure and interaction in the surfactant-dependent heat-induced gelation of protein. *Soft Matter, 20*(28), 5553–5563. https://doi.org/10.1039/D4SM00284A
Kumar, S., Kohlbrecher, J., & Aswal, V. K. (2024). Competing effects of temperature and polymer concentration on evolution of Re-entrant interactions in the nanoparticle-block copolymer system. *Langmuir, 40*(29), 14888–14899. https://doi.org/10.1021/acs.langmuir.4c00900
Kumar, S., Saha, D., & Aswal, V. K. (2023). Modifying interprotein interactions for controlling heat-induced protein gelation. *Physical Review Materials, 7*(1), Article 015601. https://doi.org/10.1103/PhysRevMaterials.7.015601
Kumar, S., Saha, D., Ray, D., Abbas, S., & Aswal, V. K. (2021). Unusual stability of protein molecules in the presence of multivalent counterions. *Physical Review E, 104*(1), Article L012603. https://doi.org/10.1103/PhysRevE.104.L012603
Kumar, S., Saha, D., Ray, D., & Aswal, V. K. (2025). Surfactant-driven modifications in protein structure. *Soft Matter, 21*, 4979–4998. https://doi.org/10.1039/D5SM00207A
Lerch, N. L., Vahedifar, A., Weiss, J., & Wu, J. (2024). Cold gelation of canola protein isolate and canola protein hydrolysates. *Food Hydrocolloids, 152*, Article 109840. https://doi.org/10.1016/j.foodhyd.2024.109840
Li, T., Senesi, A. J., & Lee, B. (2016). Small angle X-ray scattering for nanoparticle research. *Chemical Reviews, 116*(18), 11128–11180. https://doi.org/10.1021/acs.chemrev.5b00690
Liu, Z., Li, X., Guan, Z., Jia, Z., Zhang, Z., Yang, C., & Wang, J. (2024). Transglutaminase-crosslinked cold-set pea protein isolate gels modified by pH shifting: Properties, structure and formation mechanisms. *Food Hydrocolloids, 154*, Article 110158. https://doi.org/10.1016/j.foodhyd.2024.110158
Lorber, B., Fischer, F., Bailly, M., Roy, H., & Kern, D. (2012). Protein analysis by dynamic light scattering: Methods and techniques for students. *Biochemistry and Molecular Biology Education, 40*(6), 372–382. https://doi.org/10.1002/bmb.20644
Majcher, M. J., Himbert, S., Vito, F., Campea, M. A., Dave, R., Vetergaard Jensen, G., Rheinstadter, M. C., Smeets, N. M. B., & Hoare, T. (2022). Investigating the kinetics and structure of network formation in ultraviolet-photopolymerizable starch nanogel network hydrogels via very small-angle neutron scattering and small-amplitude oscillatory shear rheology. *Macromolecules, 55*(16), 7303–7317. https://doi.org/10.1021/acs.macromol.2c00874
Malkin, A. Y., Derkach, S. R., & Kulichikhin, V. G. (2023). Rheology of gels and yielding liquids. *Gels, 9*(9), 715. https://doi.org/10.3390/gels9090715
Mariz de Avelar, M. H., de Castilho Queiroz, G., & Efraim, P. (2020). Sustainable performance of cold-set gelation in the confectionery manufacturing and its effects on perception of sensory quality of jelly candies. *Cleaner Engineering and Technology, 1*. https://doi.org/10.1016/j.clet.2020.100005. Article 100005.
Mehan, S., Aswal, V. K., & Kohlbrecher, J. (2015). Tuning of protein-surfactant interaction to modify the resultant structure. *Physical Review E - Statistical Physics, Plasmas, Fluids, and Related Interdisciplinary Topics, 92*, Article 032713. https://doi.org/10.1103/PhysRevE.92.032713
Méndez-Bermúdez, J. G., & Dominguez, H. (2016). Structural changes of a sodium dodecyl sulfate (SDS) micelle induced by alcohol molecules. *Journal of Molecular Modeling, 22*(1), 33. https://doi.org/10.1007/s00894-015-2904-x
Mercadé-Prieto, R., & Gunasekaran, S. (2009). Alkali cold gelation of whey proteins. Part I: Sol−gel−sol(−gel) transitions. *Langmuir, 25*(10), 5785–5792. https://doi.org/10.1021/la804093d
Moriyama, Y., Watanabe, E., Kobayashi, K., Harano, H., Inui, E., & Takeda, K. (2008). Secondary structural change of bovine serum albumin in thermal denaturation up to 130 °C and protective effect of sodium dodecyl sulfate on the change. *The Journal of Physical Chemistry B, 112*(51), 16585–16589. https://doi.org/10.1021/jp8067624
Napieraj, M., Brûlet, A., Lutton, E., Randrianarisoa, U., Boire, A., & Boué, F. (2022). Monitoring food structure in plant protein gels during digestion: Rheometry and small angle neutron scattering studies. *Food Structure, 32*, Article 100270. https://doi.org/10.1016/j.foostr.2022.100270
Nikolaidis, A., Andreadis, M., & Moschakis, T. (2017). Effect of heat, pH, ultrasonication and ethanol on the denaturation of whey protein isolate using a newly developed approach in the analysis of difference-UV spectra. *Food Chemistry, 232*, 425–433. https://doi.org/10.1016/j.foodchem.2017.04.022
Nikolaidis, A., & Moschakis, T. (2018). On the reversibility of ethanol-induced whey protein denaturation. *Food Hydrocolloids, 84*, 389–395. https://doi.org/10.1016/j.foodhyd.2018.05.051
Nnyigide, O. S., & Hyun, K. (2020). The protection of bovine serum albumin against thermal denaturation and gelation by sodium dodecyl sulfate studied by rheology and molecular dynamics simulation. *Food Hydrocolloids, 103*, Article 105656. https://doi.org/10.1016/j.foodhyd.2020.105656
Nnyigide, T. O., Nnyigide, O. S., & Hyun, K. (2023). Rheological and molecular dynamics simulation studies of the gelation of human serum albumin in anionic and cationic surfactants. *Korean Journal of Chemical Engineering, 40*(8), 1871–1881. https://doi.org/10.1007/s11814-023-1513-0
Österberg, R., & Mortensen, K. (1994). The growth of fractal humic acids: Cluster correlation and gel formation. *Radiation and Environmental Biophysics, 33*(3), 269–276. https://doi.org/10.1007/BF01212682
Parsana, N., Kumar, S., Aswal, V. K., Seoud, O. E., & Malek, N. I. (2023). Self-healable, injectable, and conductive supramolecular eutectogel for the encapsulation and sustained release of the anticancer drug curcumin. *ACS Applied Engineering Materials, 1*(1), 380–393. https://doi.org/10.1021/acsaenm.2c00095
Pizones Ruíz-Henestrosa, V., Carrera Sánchez, C., & Rodríguez Patino, J. M. (2008). Effect of sucrose on functional properties of soy globulins: Adsorption and foam characteristics. *Journal of Agricultural and Food Chemistry, 56*(7), 2512–2521. https://doi.org/10.1021/jf0731245
Rodríguez Patino, J. M., Carrera Sánchez, C., Molina Ortiz, S. E., Rodríguez, N., Ma, R., & Añón, M. C. (2004). Adsorption of soy globulin films at the air−water interface. *Industrial & Engineering Chemistry Research, 43*(7), 1681–1689. https://doi.org/10.1021/ie0302443
Rodríguez Patino, J. M., Rodríguez Niño, M. R., & Carrera Sánchez, C. (1999). Dynamic interfacial rheology as a tool for the characterization of whey protein isolates gelation at the oil−Water interface. *Journal of Agricultural and Food Chemistry, 47*(9), 3640–3648. https://doi.org/10.1021/jf981164q
Ryu, J., & McClements, D. J. (2024). Impact of heat-set and cold-set gelling polysaccharides on potato protein gelation: Gellan gum, agar, and methylcellulose. *Food Hydrocolloids, 149*, Article 109535. https://doi.org/10.1016/j.foodhyd.2023.109535
Saha, D., Ray, D., Kohlbrecher, J., & Aswal, V. K. (2018). Unfolding and refolding of protein by a combination of ionic and nonionic surfactants. *ACS Omega 2018, 3*(7), 8260–8270. https://doi.org/10.1021/acsomega.8b00630
Sharma, R. V., & Sharma, K. C. (1977). The structure factor and the transport properties of dense fluids having molecules with square well potential, a possible generalization. *Physica A: Statistical Mechanics and its Applications, 89*(1), 213–218. https://doi.org/10.1016/0378-4371(77)90151-0
Shibayama, M. (2012). Structure-mechanical property relationship of tough hydrogels. *Soft Matter, 8*(31), 8030–8038. https://doi.org/10.1039/C2SM25325A
Shibayama, M. (2025). Physics of polymer gels: Toyoichi tanaka and after. *Soft Matter, 21*(11), 1995–2009. https://doi.org/10.1039/D4SM01418A
Shibayama, M., & Norisuye, T. (2002). Gel formation analyses by dynamic light scattering. *Bulletin of the Chemical Society of Japan, 75*(4), 641–659. https://doi.org/10.1246/bcsj.75.641
Singh, S. M., Cabello-Villegas, J., Hutchings, R. L., & Mallela, K. M. G. (2010). Role of partial protein unfolding in alcohol-induced protein aggregation. *Proteins: Structure, Function, and Bioinformatics, 78*(12), 2625–2637. https://doi.org/10.1002/prot.22778
Sokolova, A., Christoforidis, J., Eltobaji, A., Barnes, J., Darmann, F., Whitten, A. E., & de Campo, L. (2016). BILBY: time-of-flight small angle scattering instrument. *Neutron News, 27*(2), 9–13. https://doi.org/10.1080/10448632.2016.1163980
Song, W.-W., Qian, Z.-G., Liu, H., Chen, H.-F., Kaplan, D. L., & Xia, X.-X. (2021). On-Demand regulation of dual thermosensitive protein hydrogels. *ACS Macro Letters, 10*(4), 395–400. https://doi.org/10.1021/acsmacrolett.1c00062
Speroni, F., & Añón, M. C. (2013). Cold-set gelation of high pressure-treated soybean proteins. *Food Hydrocolloids, 33*(1), 85–91. https://doi.org/10.1016/j.foodhyd.2013.03.001
Stetefeld, J., McKenna, S. A., & Patel, T. R. (2016). Dynamic light scattering: A practical guide and applications in biomedical sciences. *Biophysical Reviews, 8*(4), 409–427. https://doi.org/10.1007/s12551-016-0218-6
Tobitani, A., & Ross-Murphy, S. B. (1997). Heat-induced gelation of globular proteins. 1. Model for the effects of time and temperature on the gelation time of BSA gels. *Macromolecules, 30*(17), 4845–4854. https://doi.org/10.1021/ma970112j
Tomczyńska-Mleko, M., Nishinari, K., Mleko, S., Terpiłowski, K., & Pérez-Huertas, S. (2023). Cold gelation of whey protein isolate with sugars in an ultrasound environment. *Food Hydrocolloids, 139*, Article 108510. https://doi.org/10.1016/j.foodhyd.2023.108510
Valencia, L., Nomena, E. M., Monti, S., Rosas-Arbelaez, W., Mathew, A. P., Kumar, S., & Velikov, K. P. (2020). Multivalent ion-induced re-entrant transition of carboxylated cellulose nanofibrils and its influence on nanomaterials' properties. *Nanoscale, 12*(29), 15652–15662. https://doi.org/10.1039/D0NR02888F
Venezia, V., Avallone, P. R., Vitiello, G., Silvestri, B., Grizzuti, N., Pasquino, R., & Luciani, G. (2022). Adding humic acids to gelatin hydrogels: A way to tune gelation. *Biomacromolecules, 23*(1), 443–453. https://doi.org/10.1021/acs.biomac.1c01398
Wagner, J., Andreadis, M., Nikolaidis, A., Biliaderis, C. G., & Moschakis, T. (2021). Effect of ethanol on the microstructure and rheological properties of whey proteins: Acid-induced cold gelation. *Lebensmittel-Wissenschaft & Technologie, 139*, Article 110518. https://doi.org/10.1016/j.lwt.2020.110518
Wang, T., Sun, L., Mao, X., Du, X., Liu, J., Chen, L., & Chen, J. (2023). Bridging attraction of condensed bovine serum albumin solution in the presence of trivalent ions: A SANS study. *Biochimica et Biophysica Acta (BBA) - General Subjects, 1867*(12), Article 130487. https://doi.org/10.1016/j.bbagen.2023.130487
Wignall, G. D., & Bates, F. S. (1987). Absolute calibration of small-angle neutron scattering data. *Journal of Applied Crystallography, 20*(1), 28–40. https://doi.org/10.1107/S0021889887087181
Xi, Z., Liu, W., McClements, D. J., & Zou, L. (2019). Rheological, structural, and microstructural properties of ethanol induced cold-set whey protein emulsion gels: Effect of oil content. *Food Chemistry, 291*, 22–29. https://doi.org/10.1016/j.foodchem.2019.04.011
Xu, Q., & Keiderling, T. A. (2004). Effect of sodium dodecyl sulfate on folding and thermal stability of acid-denatured cytochrome c: A spectroscopic approach. *Protein Science, 13*(11), 2949–2959. https://doi.org/10.1110/ps.04827604
Xu, Y., Sun, L., Zhuang, Y., Gu, Y., Cheng, G., Fan, X., Ding, Y., & Liu, H. (2023). Protein-stabilized emulsion gels with improved emulsifying and gelling properties for the delivery of bioactive ingredients: A review. *Foods, 12*(14), 2703. https://doi.org/10.3390/foods12142703

Yaghmur, A., Aserin, A., & Garti, N. (2002). Phase behavior of microemulsions based on food-grade nonionic surfactants: Effect of polyols and short-chain alcohols. *Colloids and Surfaces A: Physicochemical and Engineering Aspects, 209*(1), 71–81. https://doi.org/10.1016/S0927-7757(02)00168-1

Yang, C., Wang, Y., & Chen, L. (2017). Fabrication, characterization and controlled release properties of oat protein gels with percolating structure induced by cold gelation. *Food Hydrocolloids, 62*, 21–34. https://doi.org/10.1016/j.foodhyd.2016.07.023

Yoshida, K., Yamaguchi, T., Osaka, N., Endo, H., & Shibayama, M. (2010). A study of alcohol-induced gelation of β-lactoglobulin with small-angle neutron scattering, neutron spin echo, and dynamic light scattering measurements. *Physical Chemistry Chemical Physics, 12*(13), 3260–3269. https://doi.org/10.1039/B920187D

Yoshikawa, H., Hirano, A., Arakawa, T., & Shiraki, K. (2012). Effects of alcohol on the solubility and structure of native and disulfide-modified bovine serum albumin. *International Journal of Biological Macromolecules, 50*(5), 1286–1291. https://doi.org/10.1016/j.ijbiomac.2012.03.014

Yu, L., Xiong, C., Li, J., Luo, W., Xue, H., Li, R., Tu, Y., & Zhao, Y. (2020). Ethanol induced the gelation behavior of duck egg whites. *Food Hydrocolloids, 105*, Article 105765. https://doi.org/10.1016/j.foodhyd.2020.105765

Zhang, F., Roosen-Runge, F., Skoda, M. W. A., Jacobs, R. M. J., Wolf, M., Callow, P., Frielinghaus, H., Pipich, V., Prévost, S., & Schreiber, F. (2012). Hydration and interactions in protein solutions containing concentrated electrolytes studied by small-angle scattering. *Physical Chemistry Chemical Physics, 14*(7), 2483–2493. https://doi.org/10.1039/C2CP23460B

Zhao, C., Chu, Z., Miao, Z., Liu, J., Liu, J., Xu, X., Wu, Y., Qi, B., & Yan, J. (2021). Ultrasound heat treatment effects on structure and acid-induced cold set gel properties of soybean protein isolate. *Food Bioscience, 39*, Article 100827. https://doi.org/10.1016/j.fbio.2020.100827

Zhu, M., Lu, D., Milani, A. H., Mahmoudi, N., King, S. M., & Saunders, B. R. (2022). Comparing pH-responsive nanogel swelling in dispersion and inside a polyacrylamide gel using photoluminescence spectroscopy and small-angle neutron scattering. *Journal of Colloid and Interface Science, 608*, 378–385. https://doi.org/10.1016/j.jcis.2021.09.163